

AD-763 109

EFFECTS OF TURBULENCE INSTABILITIES ON
LASER PROPAGATION

David A. de Wolf

RCA Laboratories

Prepared for:

Advanced Research Projects Agency
Rome Air Development Center

April 1973

DISTRIBUTED BY:

NTIS

National Technical Information Service
U. S. DEPARTMENT OF COMMERCE
5285 Port Royal Road, Springfield Va. 22151

AD 763109

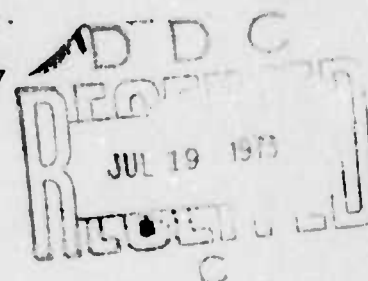
RADC-TR-73-162
Technical Report
April 1973



EFFECTS OF TURBULENCE INSTABILITIES
ON LASER PROPAGATION

RCA Laboratories

Sponsored by
Defense Advanced Research Projects Agency
ARPA Order No. 1279



Approved for public release;
distribution unlimited.

The views and conclusions contained in this document are those of the authors and should not be interpreted as necessarily representing the official policies, either expressed or implied, of the Defense Advanced Research Projects Agency or the U. S. Government.

Reproduced by
NATIONAL TECHNICAL
INFORMATION SERVICE
U.S. Department of Commerce
Springfield, VA 22151

Rome Air Development Center
Air Force Systems Command
Griffiss Air Force Base, New York

UNCLASSIFIED

Security Classification

DOCUMENT CONTROL DATA - R & D

(Security classification of title, body of abstract and indexing annotation must be entered when the overall report is classified)

1. ORIGINATING ACTIVITY (Corporate author) RCA Laboratories Princeton, N.J. 08540		2a. REPORT SECURITY CLASSIFICATION Unclassified	
		2b. GROUP N/A	
3. REPORT TITLE EFFECTS OF TURBULENCE INSTABILITIES ON LASER PROPAGATION			
4. DESCRIPTIVE NOTES (Type of report and inclusive dates) Summary Report (June 1972 to March 1973)			
5. AUTHOR(S) (First name, middle initial, last name) David A. de Wolf			
6. REPORT DATE APRIL 1973		7a. TOTAL NO. OF PAGES 1830	7b. NO. OF REFS 8
8a. CONTRACT OR GRANT NO. F30602-72-C-0486		8b. ORIGINATOR'S REPORT NUMBER(S) PRRL-73-CR-28	
b. PROJECT NO. ARPA Order No. 1279		8c. OTHER REPORT NO(S) (Any other numbers that may be assigned this report) RADC-TR-73-162	
10. DISTRIBUTION STATEMENT Approved for public release; distribution unlimited.			
11. SUPPLEMENTARY NOTES Monitored by: Capt. Darryl P. Greenwood, (315) 330-3147, RADC (OCSE) GAFB, N.Y. 13441		12. SPONSORING MILITARY ACTIVITY Defense Advanced Research Projects Agency Washington, D. C. 20301	
13. ABSTRACT A summary is given of the results up to February 1973 obtained under Contracts F30602-71-C-0356 and F30602-72-C-0486 regarding the behavior of laser beams in turbulent air. It appears important to make a distinction between focused and other beams. Amplitude scintillations appear to be unimportant in the former. Angle-of-arrival power spectra have been computed for a simple interferometer and these also contain the temporal information of focal-spot fluctuations.			

DD FORM 1473
1 NOV 65

UNCLASSIFIED

Security Classification

UNCLASSIFIED
Security Classification

14	KEY WORDS	LINK A		LINK B		LINK C	
		ROLE	WT	ROLE	WT	ROLE	WT
	Wave propagation Turbulent atmosphere, air Laser beam, focused Optics, atmospheric Irradiance fluctuations						

UNCLASSIFIED
Security Classification

EFFECTS OF TURBULENCE INSTABILITIES
ON LASER PROPAGATION

David A. de Wolf

Contractor: RCA Laboratories
Contract Number: F30602-72-C-0486
Effective Date of Contract: 15 June 1972
Contract Expiration Date: 15 August 1973
Amount of Contract: \$49,440.00
Program Code Number: 1E20

Principal Investigator: Dr. David A. de Wolf
Phone: 609 452-2700, Ext.3023

Project Engineer: Capt. Darryl P. Greenwood
Phone: 315 330-3145

Approved for public release;
distribution unlimited.

This research was supported by the
Defense Advanced Research Projects
Agency of the Department of Defense
and was monitored by Capt. Darryl P.
Greenwood, RADC (OCSE), GAFB, NY
13441 under Cont F30602-72-C-0486.

FOREWORD

The Summary Report was prepared by RCA Laboratories, Princeton, New Jersey, under Contract No. F30602-72-C-0486. It describes work performed from June 1972 to March 1973 in the Communications Research Laboratory, Dr. K. H. Powers, Director. The principal investigator and project scientist is Dr. D. A. de Wolf.

The report was submitted by the author in April 1973. Submission of the report does not constitute Air Force approval of the report's findings or conclusions. It is submitted only for the exchange and stimulation of ideas.

The Air Force Program Monitor is Captain Darryl P. Greenwood.

This technical report has been reviewed and is approved.

Darryl P. Greenwood
RADC Project Engineer

SUMMARY AND ABSTRACT

A summary is given of the results up to February 1973 obtained under Contracts F30602-71-C-0356 and F30602-72-C-0486 regarding the behavior of laser beams in turbulent air. It appears important to make a distinction between focused and other beams. Amplitude scintillations appear to be unimportant in the former. Angle-of-arrival power spectra have been computed for a simple interferometer and these also contain the temporal information of focal-spot fluctuations.

TABLE OF CONTENTS

Section	Page
SUMMARY AND ABSTRACT.	1
1. INTRODUCTION	2
2. RESULTS IN THE FOCAL PLANE OF A FOCUSED BEAM.	4
2.1 Log-Amplitude Fluctuations.	4
2.2 Focal-spot Broadening	5
2.3 Focal-spot Scintillation Rates: Power Spectrum.	7
3. RESULTS FOR COLLIMATED (PLANE-WAVE) AND DIVERGING (SPHERICAL-WAVE) BEAMS.	10
3.1 The Variance Width at $z = L$	10
3.2 Log-Amplitude Fluctuations	11
3.2.1 Weak-Amplitude Regime.	11
3.2.2 Saturation Regime.	12
3.2.3 Rayleigh Regime.	12
4. INTERFEROMETER; FEATURE RESOLUTION	13
4.1 Resolution of Features of an Illuminated Object	13
4.2 Power Spectrum of Interferometer Difference Angle-of-Arrival.	13
4.2.1 Frozen Flow ($\Delta U = 0$)	14
4.2.2 The $\omega^{-2/3}$ Portion.	15
4.2.3 Effect of the Filter Factor.	15
5. CONCLUDING REMARKS.	16
REFERENCES.	17

LIST OF ILLUSTRATIONS

Figure

1. Reduction factors for the average focal-spot area in ground-to-air propagation. Receiver at altitude Z .
2. Reduction factors for the average focal-spot area in air-to-ground propagation. Laser at altitude Z .
3. The average focal-spot area for horizontal propagation through turbulent air characterized by diverse values of C_n^2 . Note $r_L^2 = r_{Lo}^2 + r_{LB}^2$ where πr_{Lo}^2 is the free-space area of the focal spot of a Gaussian beam.
4. The normalized angle-of-arrival spectrum for two values of $\kappa_m L_o$ as a function of $\omega/f_T = L_o \omega / U_T$. Phase-difference spectral data of ref. [6] shown as heavy interrupted curve.
5. The plane-wave log-amplitude variance $\langle \chi^2 \rangle$ as a function of $\sigma_\epsilon^2 = 0.31 k^{7/6} L^{11/6} C_n^2$. A sample curve has been sketched. Note that the two abscissa points really correspond to values of $k L^2 \kappa_m^{1/3} C_n^2$ which does not differ greatly from σ_ϵ^2 .

1. INTRODUCTION

Results obtained under the contract efforts to RADC, numbered F30602-71-C-0356 and F30602-72-C-0486, in a two-year period from June 1971 to August 1973 have been reported at regular intervals in a number of reports, TRI-TRVII [1]. These results are therefore somewhat dispersed, and - moreover - several of them have required modification in later reports from earlier versions. This special report serves as a summary of most of the results obtained up to a time in early 1973, and it includes some new results yet to be reported in more detail.

The purpose of the contract effort is to analyze the degradation of laser beams in air by turbulence. Clear-air turbulence manifests itself as irregular, small variations in temperature over a large area of the ground (perhaps tens of kilometers). The refractive index is a function of temperature, and hence it fluctuates irregularly causing rays in the beam to deviate from straight-line paths. Angular fluctuations (beam wander spread), and scintillations in the image plane (blurring, distortion) are the result.

The approach of the work on these contract efforts has been to give a statistical description of these various degradations of a laser beam in terms of the statistics of the underlying refractive-index fluctuations (which in turn are given by temperature-fluctuation statistics that can be measured in principle). Thus, an atmospheric model is required. We have used the following model for homogeneous turbulence at altitude x . Let the dielectric permittivity deviate from its average (very close to unity) by an amount $\delta\epsilon(\vec{r},t)$. Define a Fourier transform of the covariance of the dielectric permittivity:

$$\Phi(K) \equiv \int d^3 \Delta r \langle \delta \mathbf{E}(\vec{r}, t) \delta \mathbf{E}(\vec{r} + \Delta r, t) \rangle \exp(i\vec{K} \cdot \Delta \vec{r}) \quad (1)$$

where \vec{r} is a point at altitude x . The atmospheric-turbulence model specifies a spectrum,

$$\Phi(K) = 32\pi^3 \times 0.033 C_n^2(x) (K^2 + L_o^{-2})^{-11/6} \exp(-K^2/\kappa_m^2), \quad (2)$$

where macroscale L_o is presumably a function of x , microscale ℓ_o is related to κ_m by the relationship $\ell_o = 5.92\kappa_m^{-1}$, and $C_n^2(x)$ is the refractive-index structure constant related to its sea-level value [2] by the relationship,

$$C_n^2(x) = C_n^2(x_o) (T_o/T)^2 (x_o/x)^{2/3} (1 + x/\ell_s)^{-2/3} \times \exp[-2(x-x_o)/h], \quad (3)$$

where $x_o \approx 1m$ and T_o are sea-level values of effective altitude and temperature, and $-7\ell_s$ is the Monin-Obukhov length ($\ell_s \rightarrow \infty$ at dawn and dusk, and $\ell_s \sim 1.5m$ at midday for well-developed turbulence). The structure function $C_n^2(z)$ can be obtained from temperature-variation measurements, and the microscale κ_m^{-1} , although harder to estimate, enters into the calculations in such a manner that an error of a factor two or so in its magnitude is not serious. The macroscale L_o varies more but it often drops out of the end result.

A useful form for the electric field of a laser beam is [3],

$$E(\vec{r}) = L^{-1} \exp[ik(L + \rho^2/2L)] \times \frac{ik}{2\pi} \int d^2 \rho_1 B(\vec{r}, \vec{r}_1) U_o(\vec{r}_1) \exp\left[\frac{ik\rho_1^2}{2} \left(\frac{1}{L} - \frac{1}{R}\right) - ik\vec{\rho} \cdot \vec{\rho}_1/L\right]. \quad (4)$$

Here $\vec{r}_1 = (\vec{\rho}_1, 0)$ is a point in the plane of the transmitting aperture,

and $\vec{r} = (\vec{\rho}, L)$ is in the plane of the receiver; $U_0(\vec{r}_1)$ is an aperture or pupil function [e.g., $\exp(-\rho_1^2/2r_0^2)$ for a Gaussian beam]; R is the radius of curvature of the phase front at $z = 0$ ($R > 0$ for a focusing beam), and $B(\vec{r}, \vec{r}_1)$ is the ratio of the electric field in turbulent air at \vec{r} due to a point source at \vec{r}_1 to a similar field in free space. This expression requires $kL \gg 1$ (radiation-zone condition), $L \ll kr_0^2$ (near field of the aperture), and a sagittal condition $kr_0^4 \ll L^3$, all of which usually hold, and it is restricted also to points \vec{r} such that $k\rho^4 \ll L^3$, which is sufficiently liberal to include all points of interest in the image plane when propagation distances exceed a few hundred meters.

Our work shows that the effect of atmospheric turbulence upon laser beams is importantly different in the focal plane of an optimally focused beam from the effect upon collimated-beam and diverging-beam images. It makes sense to distinguish the case of a focused beam from the others because there appear to be only negligible amplitude effects in the former. A strong case can be made that the focal image of a focused beam is determined by free-space diffraction effects upon which ray bending due to turbulence is superimposed. Ensuing results are discussed in the next section.

2. RESULTS IN THE FOCAL PLANE OF A FOCUSED BEAM

2.1. Log-Amplitude Fluctuations

The electric field in the focal plane of a focused beam is given by Eq. (4) in the special case $R = L$. For a Gaussian beam in free space, Eq. (4) yields [3],

$$E_c(\vec{r}) = \frac{-ikw^2}{L-ikw^2} \exp\{ik[L + \rho^2/2(L-ikw^2)]\}$$

$$w^{-2} = r_o^{-2} + ik/R \quad (5)$$

Using methods of our own that lead to an intermediate result equivalent to Eqs. (28) and (29) of Ishimaru [4] we find a log-amplitude variance for a Gaussian beam:

$$\langle x_{gb}^2 \rangle \approx 0.102 (L/kr_o^2)^{7/6} \times (C_n^2 k^{7/6} L^{11/6}) \quad (6)$$

The constant in Eq. (6) is $(0.033\pi^2/12) \times \Gamma(3)\Gamma(2/3)/\Gamma(11/3) \approx 0.102$.

The important point is that $L \ll kr_o^2$ for all cases of interest (whereas $0.31C_n^2 k^{7/6} L^{11/6}$ appears never to exceed a value of the order of 10), and therefore $\langle x_{gb}^2 \rangle \ll 1$. Thus, amplitude fluctuations do not contribute appreciably to the effects in the focal plane.

2.2. Focal-spot Broadening

The previous result strongly suggests that the image in the focal spot is distorted by undulations in the rays directed by the mirror toward a focal spot. There are many different ways to define variables for the broadening. Some of these are discussed in TRI and TRIV. In our view, the most fundamental (although not necessarily the most practical) one is the variance width r_{LB}^2 . Consider the normalized average intensity $i(\vec{\rho}) = \langle I(\vec{\rho}, L) / \int d^2 \rho I(\vec{\rho}, L) \rangle$. The variance width r_L^2 is then defined as

$$r_L^2 \equiv \int d^2 \rho \rho^2 i(\vec{\rho}) - [\int d^2 \rho \rho i(\vec{\rho})]^2 \quad (7)$$

The quantity r_{Lo}^2 is defined likewise in terms of the normalized free-space intensity $i_o(\vec{\rho})$ equivalent in definition to $i(\vec{\rho})$ if $\langle I(\vec{\rho}, L) \rangle$ is

replaced by $I_0(\rho, L)$. We finally define $r_{LB}^2 \equiv r_L^2 - r_{Lo}^2$, and find:

$$r_{LB}^2 = 12\pi^2 \times 0.033 L^2 K_m^{1/3} \int_0^L ds s^2 C_n^2(s) \quad (8)$$

for an axial path from $s = 0$ to $s = L$. For a homogeneous path one finds $r_{LB}^2 \approx 1.3 L^3 K_m^{1/3} C_n^2$. The significance of this result, which may be somewhat difficult to compare in detail to data because it requires much processing of data, is that it is a very fundamental and general result, independent of beam shape, aperture function, etc., and it holds even when r_L^2 and r_{Lo}^2 are not finite in which case it can be obtained from data by forming,

$$r_{LB}^2 \equiv \int_0^{\rho_N} d^2 \rho \rho^2 [i(\vec{\rho}) - i_o(\vec{\rho})] \quad (9)$$

where ρ_N is a radius value beyond which the intensity drops below the noise. The quantity r_{LB}^2 represents an area that expresses a displacement of energy away from the central axis into the sides by turbulence-induced refraction. This view is supported by looking at the radial displacement $r_{LB}' \equiv L\theta$ where θ is the angular deviation of a ray pointed initially at the focal point from some location on the mirror and deflected randomly and slowly by refractive-index fluctuations. It is easily seen that $\langle \theta \rangle = 0$ and $\langle \theta^2 \rangle = 1.3 L K_m^{1/3} C_n^2$ for a homogeneously turbulent medium, as a consequence of which it follows that $\langle (r_{LB}')^2 \rangle = r_{LB}^2$. This result, coupled with Eq. (6), suggests a simplified model for the instantaneous intensity in the focal plane that will be considered in future work.

Equation (8) has been worked out for air-to-ground propagation as well as for the opposite case (unfortunately, the results in TRIV have

been interchanged for those two cases). In both cases, we name the resulting variance width $r_{LB}^2(Z)$ where Z is the height of the receiver (ground-to-air case) or of the transmitter (air-to-ground case). It is compared to $r_{LB}^2(0)$: the horizontal-propagation case. The following table summarizes results for the ratio $r_{LB}^2(Z)/r_{LB}^2(0)$:

TABLE I: $r_{LB}^2(Z)/r_{LB}^2(0)$		
	Sunny Day	Dawn, Dusk
Ground -To-Air	$9x_o^{1/3} \ell_s^{1/3} Z^{-1}$	$9(x_o/Z)^{2/3}$
Air-To -Ground	$1.8(x_o \ell_s)^{2/3} Z^{-4/3}$	$1.3(x_o/Z)^{2/3}$

These formulas are approximations for altitude Z much less than h (see Eq. (3) for explanation of ℓ_s and x_o). The inverse ratio has been plotted in Figs. 1 and 2 for appropriate choices of ℓ_s (1.5 m or ∞) and x_o (1 m). The calculations have been performed by inserting Eq. (3) into Eq. (8), and they include some corrections of the original presentation. The ground-level variance width $r_{LB}^2(0) \equiv r_{LB}^2$ has been plotted in Fig. 3 for several values of C_n^2 . Fig. 3 also includes two plots of $r_{Lo}^2 = (L/kr_o)^2$, the variance width of the free-space focal spot of a diffraction-limited Gaussian beam, for comparison. It indicates the significance of the broadening.

2.3. Focal-spot Scintillation Rates: Power Spectrum

The variance width r_{LB}^2 , defined in (7), can be made into a covariance function with respect to time (thus to yield information on scintillation

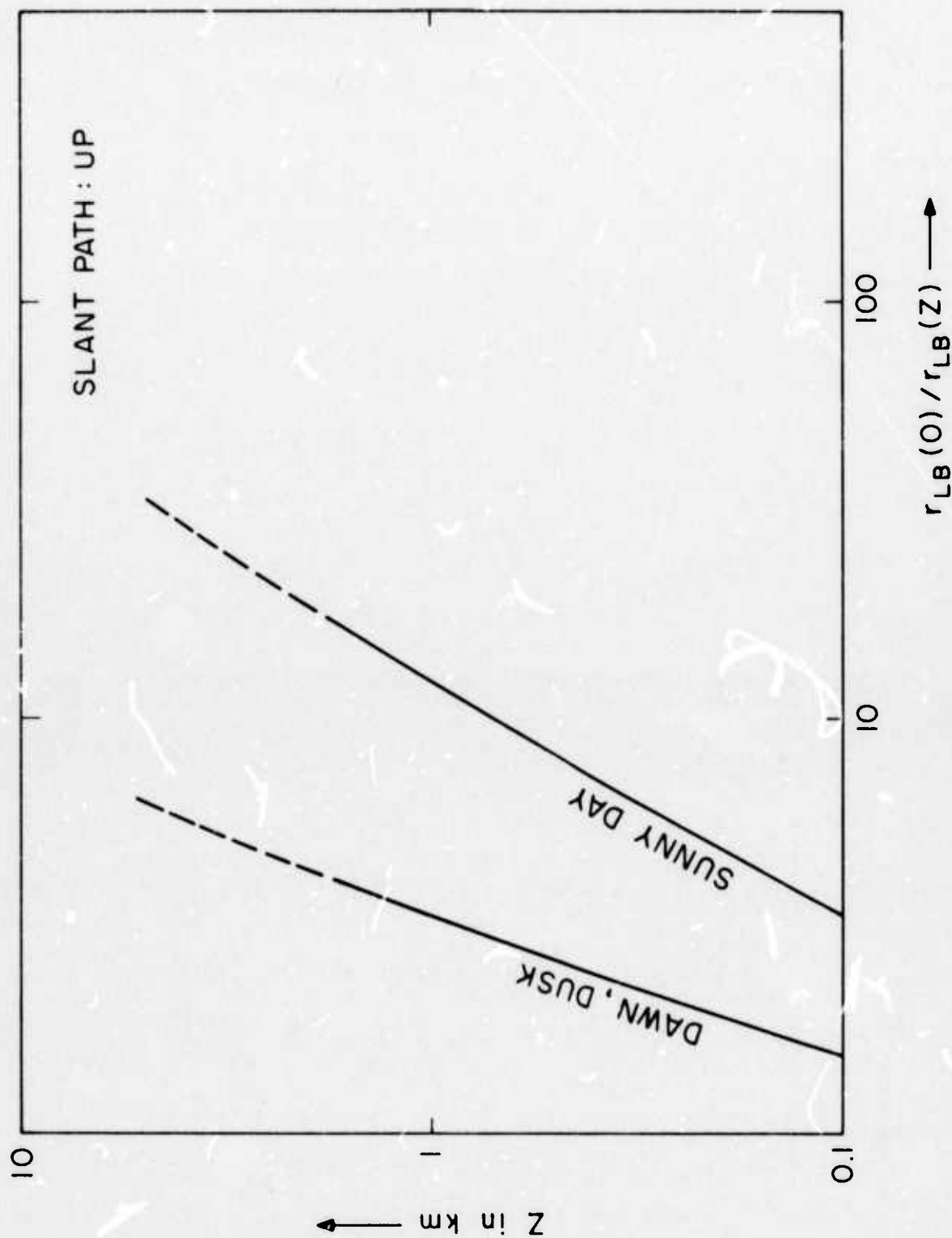


Figure 1. Reduction factors for the average focal-spot area in ground-to-air propagation. Receiver at altitude Z .

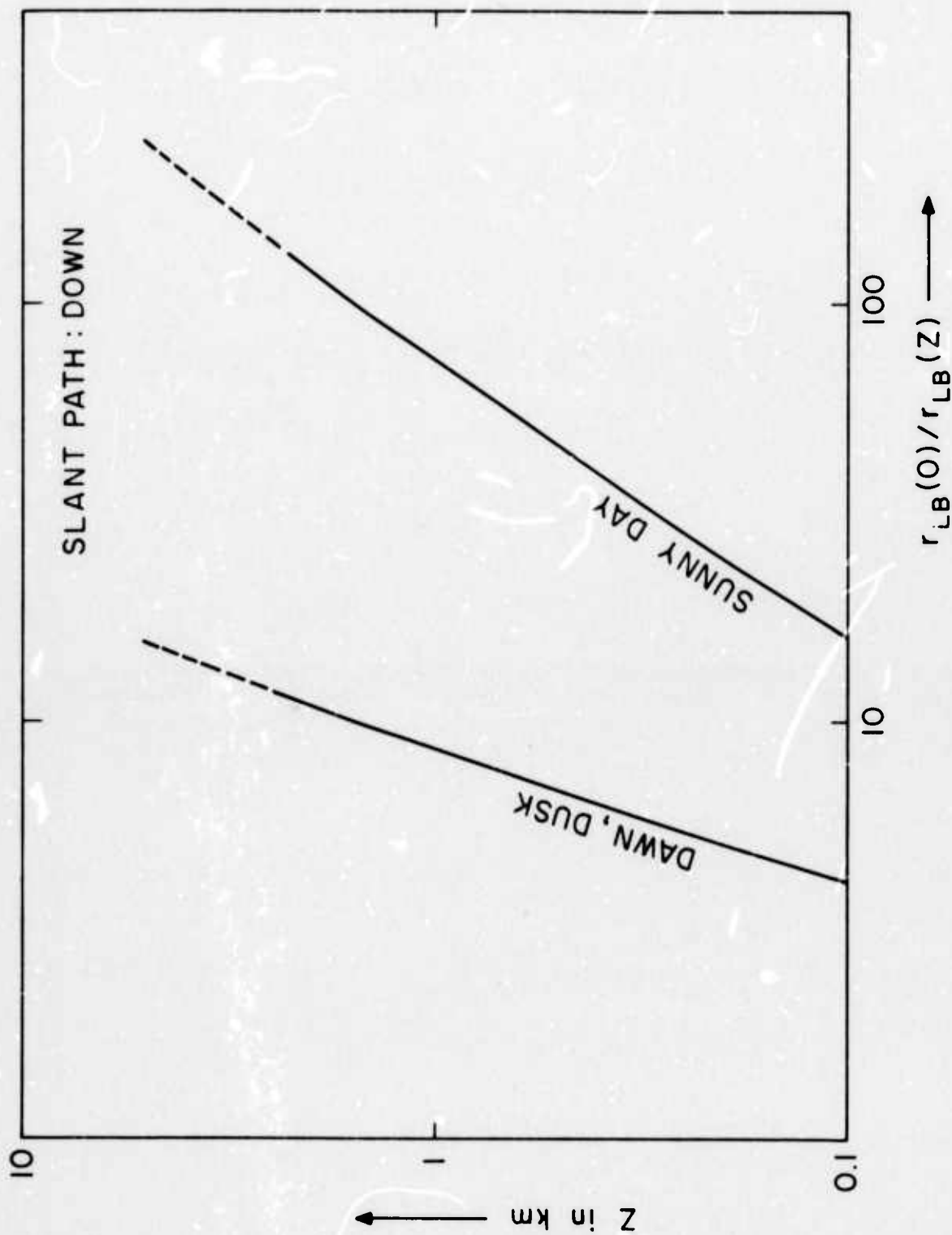


Figure 2. Reduction factors for the average focal-spot area in air-to-ground propagation. Laser at altitude Z .

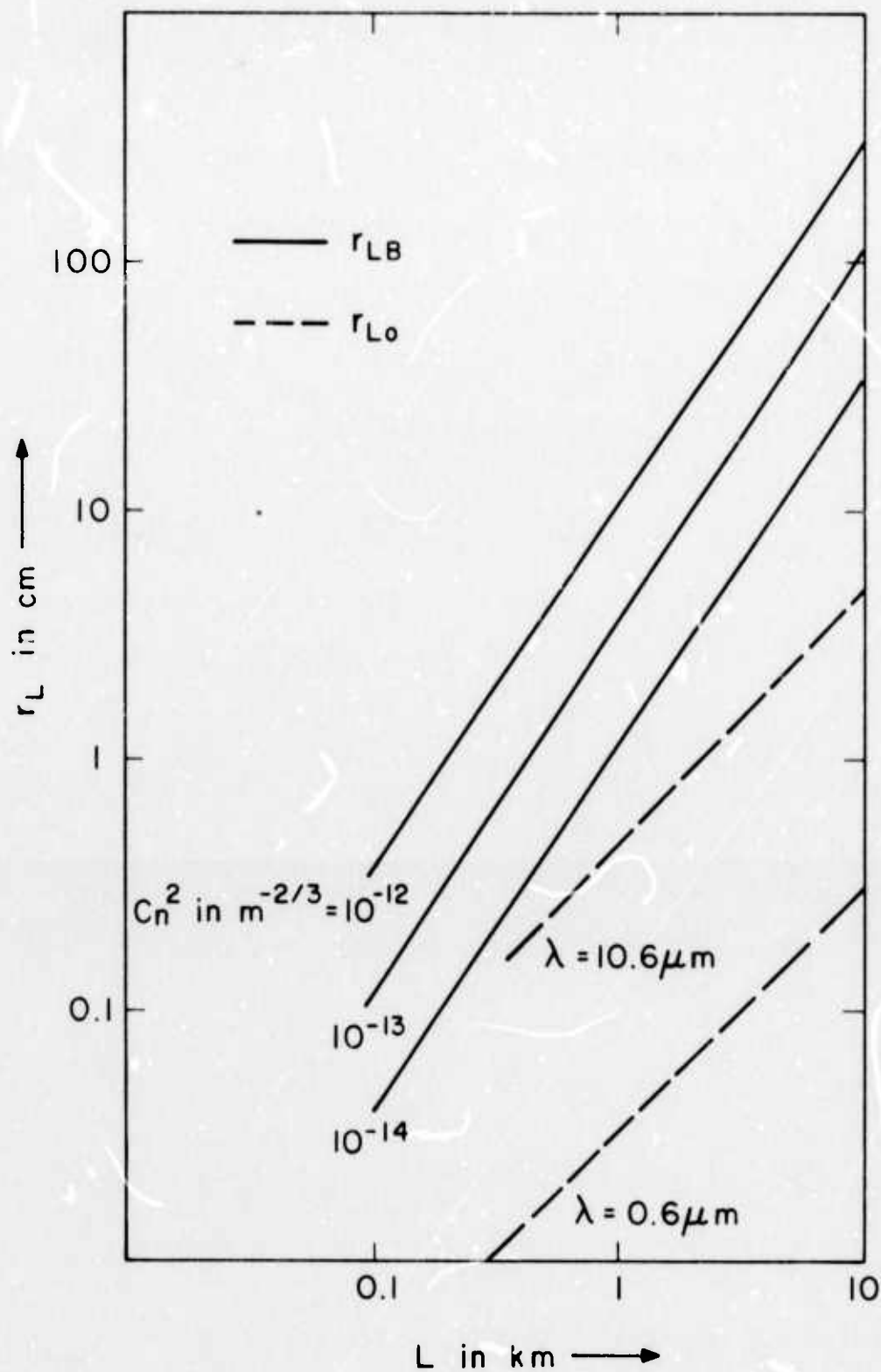


Figure 3. The average focal-spot area for horizontal propagation through turbulent air characterized by diverse values of C_n^2 . Note $r_L^2 = r_{Lo}^2 + r_{LB}^2$ where πr_{Lo}^2 is the free-space area of the focal spot of a Gaussian beam.

rates) by redefining

$$r_{LB}^2(\tau) \equiv \int d^2 \rho \rho^2 [\langle E(\vec{r}, t) E^*(\vec{r}, t + \tau) \rangle - I_0(\vec{r})] / \int d^2 \rho \langle I(\vec{r}) \rangle . \quad (10)$$

Note that the first moments are ignored (asymmetric beams are not considered). For a homogeneously turbulent medium, it can be seen that

$$r_{LB}^2(\tau) = L^2 \langle \theta(t) \theta(t + \tau) \rangle \quad (11)$$

where $\theta(t)$ is the angular deviation of a ray. Thus, the Fourier transform of $r_{LB}^2(\tau)$ yields the power spectrum of either the square root of the focal-spot variance width, or - equivalently - of the transverse deviation of a ray. The power spectrum $W_\theta(\omega) d\omega$ tells you how this variance is apportioned into contributions with fluctuation rates lying between ω and $\omega + d\omega$. It has been computed for turbulence characterized by a random Gaussian distribution of velocities with mean \vec{U} and variance ΔU^2 . Only the transverse components U_T of \vec{U} and $2\Delta U^2/3$ enter into the calculations. The results are lengthy and some preparation is needed to write them down. The velocities U_T , ΔU , and the scales L_0 , ℓ_0 define four frequencies

$$\begin{aligned} \omega_T &= U_T / L_0 , & \Delta\omega &= 4\Delta U / L_0 \sqrt{3} \\ \Omega_T &= \kappa_m U_T , & \Delta\Omega &= 4\kappa_m \Delta U \sqrt{3} \end{aligned} \quad (12)$$

For the turbulence spectrum of Eq. (2) we find the following power spectrum:

$$W_\theta(\omega) = 4\pi^2 \times 0.033 C_n^2 L_0^{-1/3} [W_\theta(\omega, 5/6) - W_\theta(\omega, 11/6)] \quad (13)$$

The forms for $W_\theta(\omega, q)$ can be found from Tables II and III, and they can be adopted to Eq. (13) by setting $q = 11/6$ and subtracting the resulting form from that for $q = 5/6$. A normalized form of the spectrum based

TABLE II: ANGLE-OF-ARRIVAL POWER SPECTRUM
FOR FROZEN FLOW ($\Delta U=0$)

$W_{\theta}(\omega, q)$

$\frac{\sqrt{\pi}}{\omega_T} \left(1 + \omega^2/\omega_T^2\right)^{1/2-q} e^{-\omega^2/\Omega_T^2} U[1/2, 3/2-q, (\omega^2 + \omega_T^2)/\Omega_T^2]$		
$\frac{\Gamma(q-1/2)}{\Gamma(q)} \frac{\sqrt{\pi}}{\omega_T} \left(1 + \omega^2/\omega_T^2\right)^{1/2-q} e^{-\omega^2/\Omega_T^2}$		$\frac{\sqrt{\pi}}{\omega_T} \frac{\Omega_T}{\omega_T} (1 + \omega^2/\omega_T^2)^{-q} e^{-\omega^2/\Omega_T^2}$
$\frac{\Gamma(q-1/2)}{\Gamma(q)} \frac{\sqrt{\pi}}{\omega_T}$	$\frac{\Gamma(q-1/2)}{\Gamma(q)} \frac{\sqrt{\pi}}{\omega_T} \left(\frac{\omega}{\omega_T}\right)^{1-2q}$	$(\kappa_m L_o) \frac{\sqrt{\pi}}{\omega_T} \left(\frac{\omega}{\omega_T}\right)^{-2q} e^{-\omega^2/\Omega_T^2}$

$$\omega_T = U_T/L_o$$

$$\Omega_T = \kappa_m U_T$$

$\omega \rightarrow$

TABLE III: ANGLE-OF-ARRIVAL POWER SPECTRUM
FOR RANDOM FLOW ($U_T=0$)

$W_{\theta}(\omega, q)$

$\frac{\sqrt{\pi}}{\Delta\omega} \Gamma(q-1/2) U(q-1/2, 1/2 \omega^2/\Delta\omega^2)$		
	$\frac{\sqrt{\pi}}{\Delta\omega} 2(\kappa_m L_o \omega/\Delta\omega)^{1/2-q} K_{q-1/2}(2\omega/\Delta\Omega)$	
$\frac{\Gamma(q-1/2)}{\Gamma(q)} \frac{\pi}{\Delta\omega}$	$\Gamma(q-1/2) \left(\frac{\sqrt{\pi}}{\Delta\omega}\right)^{1-2q} \frac{\omega}{\Delta\omega}$	$(\kappa_m L_o) \frac{\pi}{\Delta\omega} \left(\frac{2\omega}{\Delta\Omega}\right)^{-q} e^{-2\omega/\Delta\Omega}$

$$\Delta\omega \sim \Delta U/L_o$$

$$\Delta\Omega \sim \kappa_m \Delta U$$

$\omega \rightarrow$

on Table II is plotted in Fig. 4 for $\kappa_m L_o = 100$ and $\kappa_m L_o = 1000$. All frequencies denoted by letter "f" in this plot can also be considered as angular frequencies ω .

The power spectrum has a flat portion for low frequencies, followed by a transition to an $\omega^{-2/3}$ portion, which in turn is followed by a rapid decay. The $\omega^{-2/3}$ portion is presumably the only significant part of the spectrum because the lower-frequency portion assumes the absence of large-scale fluctuations, and the high-frequency fall-off is dependent in detail upon the exponential tail of Eq. (2): an approximate description which suffices for most other applications but not for this one. The following approximation of $W_\theta(\omega, 5/6)$ appears to yield a useful expression whenever ω exceeds the maximum of ω_T and $\Delta\omega$:

$$W_\theta(\omega, 5/6) \approx \Gamma(1/3) \frac{\sqrt{\pi}}{\Delta\omega} \left(\frac{\omega}{\Delta\omega}\right)^{-2/3} {}_1F_1(1/6, 1, -\omega_T^2/\Delta\omega^2) \quad , \quad (14)$$

where ${}_1F_1$ is a confluent hypergeometric function in a well-known notation [7]. An asymptotic expansion for small $\Delta\omega/\omega_T$ is probably sufficient for all cases except those where $U_T \approx 0$.

The spectrum in Fig. 4 has been tested with Russian data [6] shown in a thick interrupted line. These are phase-difference data, not angle-of-arrival data, and therefore agreement is good only for $f < U_T/d$ where d is the separation. For these data, that implies $f/f_T < 10$.

3. RESULTS FOR COLLIMATED (PLANE-WAVE) AND DIVERGING (SPHERICAL-WAVE) BEAMS

3.1. The Variance Width At $z = L$

For a Gaussian beam described by (5), one can recompute Eq. (7)

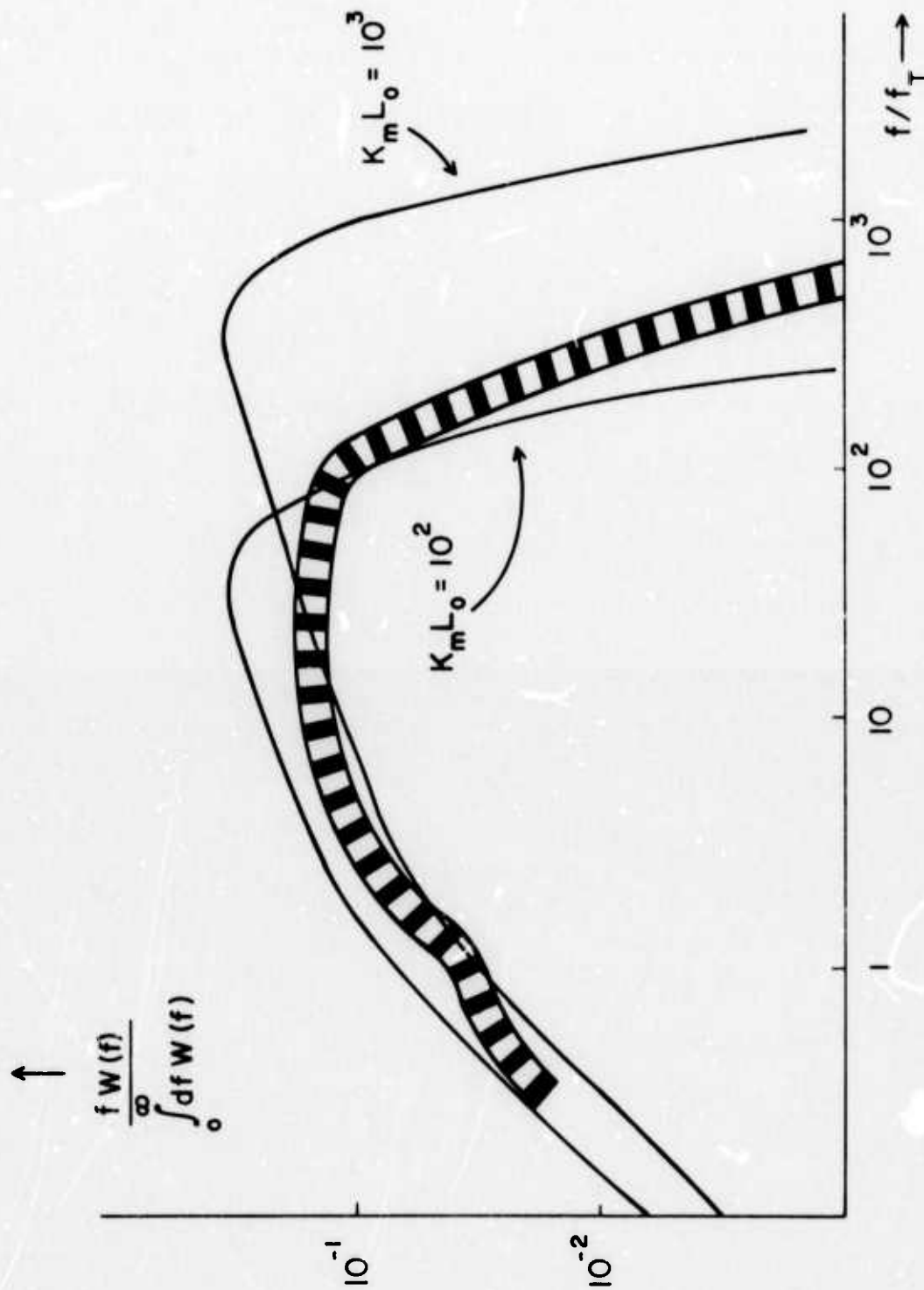


Figure 4. The normalized angle-of-arrival spectrum for two values of $K_m L_o$ as a function of $f/f_T = L_o \omega / U_T$. Phase-difference spectral data of ref. [6] shown as heavy interrupted curve.

to find:

$$r_L^2 = r_o^2 [(1-z/R)^2 + (z/kr_o^2)^2] + r_{LB}^2, \quad (15)$$

i.e., the variance width in any plane at an appreciable distance from the laser is the Pythagorean sum of the width r_{LB} solely determined by atmospheric turbulence and a width r_{Lo} characteristic of the beam in free space. At $z = R$, Eq. (15) reduces to the focused-beam case in the focal plane depicted in Fig. 3. For a collimated beam, it reduces to $r_L^2 \approx r_o^2 + r_{LB}^2$, and for a diverging beam to $r_L^2 \approx r_o^2 (R + Z)^2/R^2 + r_{LB}^2$. Thus for wide beams, or for diverging beams, the broadening effect is much less important than it is in the focal plane of a focused beam. The internal structure of the large spot at $z = L$ is now of much greater importance, and it appears to be determined mainly by amplitude fluctuations: in strong contrast to the focused-beam case.

3.2. Log-amplitude Fluctuations

The analysis of amplitude fluctuations - probably the dominant mechanism of image distortion in diverging beams - is extremely difficult. The following results have been obtained, and they are illustrated in Fig. 5 for plane waves (the illustration for spherical waves would be quite similar).

3.2.1. Weak-amplitude regime

The amplitude fluctuations are log-normally distributed with zero log-amplitude mean, and with

$$\langle I^N \rangle = I_o^N \exp[2N(N-1)\langle x^2 \rangle] \quad (16)$$

where,

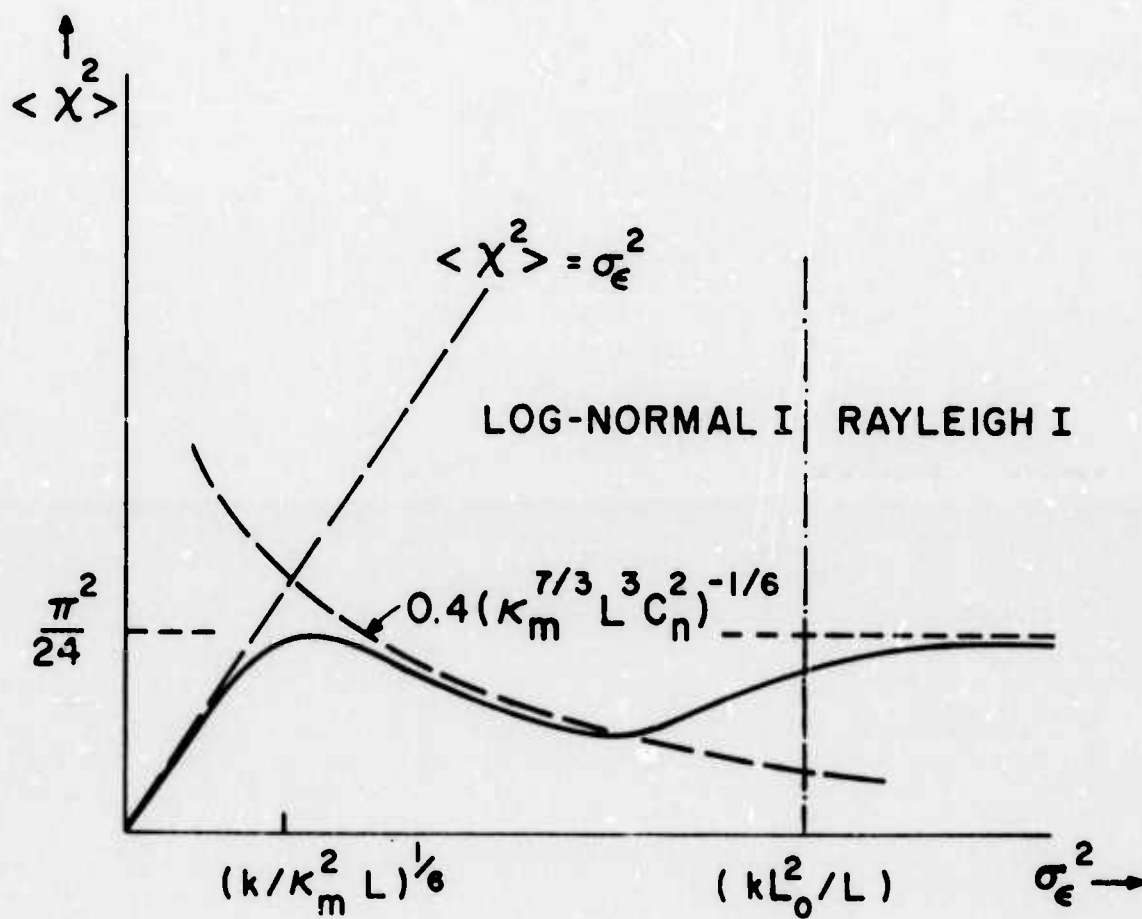


Figure 5. The plane-wave log-amplitude variance $\langle \chi^2 \rangle$ as a function of $\sigma_\epsilon^2 = 0.31k^{7/6}L^{11/6}C_n^2$. A sample curve has been sketched. Note that the two abscissa points really correspond to values of $kL^2\kappa_m^{1/3}C_n^2$ which does not differ greatly from σ_ϵ^2 .

$$\begin{aligned}\langle \chi^2 \rangle &\approx 0.307 k^{7/6} L^{11/6} C_n^2 : \text{ plane waves} \\ \langle \chi^2 \rangle &\approx 0.124 k^{7/6} L^{11/6} C_n^2 : \text{ spherical waves}\end{aligned}\quad (17)$$

These modified-Rytov results appear to be valid whenever the variance of the ray-angle deviation $\kappa_m^{1/3} L C_n^2$ is much less than the square of the Fresnel angle $(kL)^{-1/2}$, i.e., $kL^2 \kappa_m^{1/3} C_n^2 \ll 1$.

3.2.2. Saturation regime

As the parameter $kL^2 \kappa_m^{1/3} C_n^2$ exceeds unity, i.e., when ray bending starts to lead to interference effects with undeflected rays, the variances in Eqs. (17) are no longer small compared to unity and Eqs. (17) are no longer valid. This parameter regime is quite relevant to laser-beam propagation over kilometer paths. New results indicate that the amplitude is asymptotically log-normal, i.e., Eq. (16) holds asymptotically. Recent results by other workers [5] indicate that the amplitude cannot be exactly log-normal; however, an asymptotic result seems reasonable at present, and Eqs. (17) must then be replaced by,

$$\begin{aligned}\langle \chi^2 \rangle &\approx 0.41 (\kappa_m^{7/3} L^3 C_n^2)^{-1/6} : \text{ plane waves} \\ \langle \chi^2 \rangle &\approx 1.25 (\kappa_m^{7/3} L^3 C_n^2)^{-1/6} : \text{ spherical waves}\end{aligned}\quad (18)$$

Thus, the amplitude fluctuations have peaked somewhere at $\kappa_m^{1/3} L C_n^2 \sim (kL)^{-1}$, and now decrease with increasing L and C_n^2 .

3.2.3. Rayleigh regime

The decrease does not continue ad infinitum because when $kL^2 \kappa_m^{1/3} C_n^2$ approaches and exceeds the Fresnel number kL_o^2/L , the amplitude becomes Rayleigh distributed, i.e.,

$$\langle I^N \rangle = N! I_o^N \quad (19)$$

This is a limit never observed with laser beams, because the above criterion means that rays are refracted laterally by more than a macroscale L_0 , and that is very unlikely for beams propagating even tens of kilometers through turbulent air.

4. INTERFEROMETER; FEATURE RESOLUTION

4.1. Resolution Of Features Of An Illuminated Object

A simple study has led to a criterion for distinguishing two features separated by an angle $\theta_g = \rho_o/L$ on an object at distance L from the observer in the presence of turbulent air. Complete absence of other noise has been assumed so that perfect resolution at any angle in free space is assumed. The criterion expresses the magnitude of the variation $\delta\theta$ in the difference of two rays to the eye coming from each point feature. It reads

$$\begin{aligned} \langle (\delta\theta/\theta_g)^2 \rangle &\approx (r_{LB}/0.61\ell_o)^2 \quad \text{for } \rho_o \ll \ell_o \\ &\approx (2.4r_{LB}/\rho_o)^2 \quad \text{for } \rho_o \gg \ell_o \end{aligned} \quad (20)$$

Thus, small separations compared to ℓ_o are either obscured ($r_{LB} > \ell_o$) or they are not. Larger separations can be resolved or not, depending upon the size of r_{LB} (to be read off from Fig. 3 for horizontal propagation). Slant-path propagation requires some modification factors, namely,

$$\begin{aligned} \langle \delta\theta^2(z) \rangle / \langle \delta\theta^2 \rangle &\approx 5(z_o/z) && : \text{ sunny day} \\ &\approx 3(z_o/z)^{2/3} && : \text{ dawn, dusk} \end{aligned} \quad (21)$$

for an object at altitude Z .

4.2. Power Spectrum Of Interferometer Difference Angle-Of-Arrival

Finally, a simple application and extension of the results of sec-

tion 2.3 are to be found in examining the difference angle of arrival of a simple interferometer consisting of two parallel rays separated by a distance ρ . This angle is a measure of the distortion of an image, whereas the half-sum angle expresses a lateral shift of the image. The power spectrum for this case has a form similar to Eq. (13), namely

$$W_{\delta\theta}(\omega) = 8\pi^2 \times 0.033 C_n^2 L_0^{-1/3} [W_{\delta\theta}(\omega, 5/6) - W_{\delta\theta}(\omega, 11/6)] . \quad (22)$$

The difference lies in the form of $W_{\delta\theta}$,

$$W_{\delta\theta}(\omega, q) = W_{\theta}(\omega, q) F_{\rho}(\omega, q) , \quad (23)$$

which differs from the single-ray function $W_{\theta}(\omega, q)$ by inclusion of a filter factor. Some extra definitions are required in order to give the filter factor. Let φ be the angle in the x-y plane between transverse average velocity \vec{U}_T and separation vector $\vec{\rho}$. Define

$$\begin{aligned} \xi_c &= \rho \cos \varphi / L_0 \\ \xi_s &= \rho \sin \varphi / L_0 \end{aligned} \quad (24)$$

The following forms have been found for the filter factor $F_{\rho}(\omega, q)$:

4.2.1. Frozen Flow ($\Delta U = 0$)

$$\begin{aligned} F_{\rho}(\omega, q) &= 1 - \sum_{m=0}^{\infty} \cos(\xi_c \omega / \omega_T) \frac{1}{m!} [-(\xi_s^2/4)(1 + \omega^2/\omega_T^2)]^m \\ &\times \frac{U[1/2 + m, 3/2 - q + m, (\omega^2 + \omega_T^2)/\Omega_T^2]}{U[1/2, 3/2 - q, (\omega^2 + \omega_T^2)/\Omega_T^2]} \end{aligned} \quad (25)$$

where $U(a, b, z)$ is the Kummer function of formula (13.1.33) of Ref. [7].

If the dissipation range of turbulence is excluded, i.e., $\omega \ll \Omega_T$, Eq.

(25) is considerably simplified to:

$$F_{\rho}(\omega, q) = 1 - \frac{2^{3/2-q}}{\Gamma(q-1/2)} \cos(\xi_c \omega / \omega_T) (1 + \omega^2 / \omega_T^2)^{q/2-1/4} \xi_s^{-1/2} \quad (26)$$

$$\times K_{1/2-q} [\xi_s (1 + \omega^2 / \omega_T^2)^{1/2}]$$

4.2.2. The $\omega^{-2/3}$ portion

Analogous to Eq. (14), we are able to work out a general expression for the inertial subrange of the power spectrum, that is most useful when $\Delta U \ll U_T$. Only the $q = 5/6$ filter factor will be given to correspond with Eq. (14) according to the recipe of Eq. (22): the $q = 11/6$ factor can be given but it appears superfluous to do so:

$$F(\omega, 5/6) = 1 - \frac{2 \cos \xi_c \omega / \omega_T}{\Gamma(1/3)} \sum_{m=0}^{\infty} \frac{1}{m!} (\xi_s \omega / 2 \omega_T)^{m+1/3} \quad (27)$$

$$\times K_{m-1/3}(\xi_s \omega / \omega_T) \frac{{}_1F_1(1/6+m, 1, -\omega_T^2 / \omega^2)}{{}_1F_1(1/6, 1, -\omega_T^2 / \omega^2)}$$

The flat portion of the spectrum (for very small ω) can also be given - see TRVI, section 4.2.2 - but it is not worth repeating here because it is probably only a formal result without much physical significance.

4.2.3. Effect of the filter factor

Equations (25)-(27) are, perhaps unnecessarily, complicated, but their content can be stated more simply in qualitative terms. Just consider the cases where $F_{\rho}(\omega, q)$ reduces either to $F_{\rho} \approx 1$ or $F_{\rho} \approx 0$. In the case that $\xi_c \approx 0$, i.e., that the plane of the interferometer is perpendicular to the crosswind, it follows from Eq. (26) that $F_{\rho} \approx 1$ for frequencies well into the $\omega^{-2/3}$ region. Thus, for a vertical interferometer, the filter factor is important only at low frequencies. On the other hand, for a horizontal interferometer, i.e., $\xi_s \approx 0$, the filter factor reduces to $1 - \cos(\xi_c \omega / \omega_T)$ for all except the very highest frequencies (depending upon how non-zero ξ_s really is). The filter factor then filters

out of the spectrum the resonance frequencies $\omega = 2\pi n\omega_T/\xi_c = 2\pi nU_T/\rho \cos\phi \approx 2\pi nU_T/\rho$, but does not otherwise affect the spectrum.

5. CONCLUDING REMARKS

The preceding sections 2-4 summarize the most important results of the contract effort to date. In summary, it appears that a focused beam produces an image spot in turbulent air that is determined by free-space diffraction interference and turbulence-induced angular refraction effects. This result is expressed by Eq. (6) for negligible turbulence-induced amplitude fluctuations, and by Eq. (8) for the average area broadening of the focal spot. The latter broadening corresponds exactly to a broadening due to angular refraction of rays only. Table I expands Eq. (8) to the case of slant paths. Thus the quantity determining the broadening of the focal spot is in essence the lateral deviation of a randomly refracted ray. The power spectrum associated with both of these is one and the same quantity and it is given by Eqs. (13), (14), and Tables II and III. The power spectrum subdivides a variance (in this case of either the focal radius or the lateral deviation of a ray) into frequency components; each component corresponding to fluctuations at a given frequency. It contains all the information on fluctuation rates.

Strongly diverging or wide collimated beams, on the other hand, produce images in which amplitude fluctuations are also of importance, particularly in the interior of the spot. This information is not contained in the mutual-coherence factor, apparently, because the mcf is determined solely by phase fluctuations. Equations (16)-(19) give results for amplitude fluctuations. Not included in these results are

the effects of intermittency: these will be reported at a later date.

Some simple criteria for resolution of features of an image in turbulent (but otherwise noise-free) air are given in Eqs. (20)-(21). As expected, these criteria revolve around angular-deviation parameters.

Finally, the power spectrum of a simple interferometer difference - angle of arrival is computed in Eqs. (25), (26), and (27), and related to the angle-of-arrival power spectrum. These results complement those of Reinhardt and Collins [8] for phase-difference spectra.

The results appear to contain much information. A power spectrum, for instance, probably contains much more information than one really requires for understanding the rates at which fluctuations occur. One of the tasks of the immediate future will be to extract pertinent information from these many results.

REFERENCES

- [1] D. A. de Wolf, Technical and Final Reports to Rome Air Development Center on "Effects of Turbulence Instabilities on Laser Propagation" under Contracts No. F30602-71-C-0356 (July 1971 - June 1972) and No. F30602-72-C-0486 (June 1972 - December 1972):
- RADC-TR-71-249, October 1971, TRI
- RADC-TR-72-32, January 1972, TRII
- RADC-TR-72-51, February 1972, TRIII
- RADC-TR-72-119, April 1972, TRIV
- RADC-TR-72-204, July 1972, TRV

RADC-TR-72-308, October 1972, TRVI

RADC-TR-73-33, January 1973, TRVII

- [2] J. C. Wyngaard, Y. Izumi, and S. A. Collins, Jr., J. Opt. Soc. Am. 61, 1646 (1971).
- [3] R. A. Schmeltzer, Quart. Appl. Math. 24, 339 (1966).
- [4] A. Ishimaru, Proc. IEEE 57, 407 (1969).
- [5] J. W. Strohbehn and T. I. Wang, Paper Tu116 at 1973 Spring Meeting Opt. Soc. Am. Denver, Colo. March 13-16.
- [6] A. S. Gurvich, M. A. Kallistratova, and N. S. Time, Izv. Vuz Radiofizika (Radiophysics and Quantum Electronics) 11, 1360 (1968).
- [7] M. Abramowitz and I. A. Stegun, Handbook of Mathematical Functions, NBS Applied Mathematics Series 55 (U.S. Government Printing Office, Washington, D. C.; June 1964).
- [8] G. W. Reinhardt, and S. A. Collins, Jr., J. Opt. Soc. Am. 62, 1526 (1972).